NANO · MICRO small
www.small-journal.com

Soybean Lecithin-Mediated Nanoporous PLGA Microspheres with Highly Entrapped and Controlled Released BMP-2 as a Stem Cell Platform

*Daixu Wei, Ruirui Qiao, Jinwei Dao, Jing Su, Chengmin Jiang, Xichang Wang, Mingyuan Gao, and Jian Zhong**

Injectable polymer microsphere-based stem cell delivery systems have a severe problem that they do not offer a desirable environment for stem cell adhesion, proliferation, and differentiation because it is difficult to entrap a large number of hydrophilic functional protein molecules into the core of hydrophobic polymer microspheres. In this work, soybean lecithin (SL) is applied to entrap hydrophilic bone morphogenic protein-2 (BMP-2) into nanoporous poly(lactide-co-glycolide) (PLGA)-based microspheres by a two-step method: SL/BMP-2 complexes preparation and PLGA/SL/BMP-2 microsphere preparation. The measurements of their physicochemical properties show that PLGA/SL/BMP-2 microspheres had significantly higher BMP-2 entrapment efficiency and controlled triphasic BMP-2 release behavior compared with PLGA/BMP-2 microspheres. Furthermore, the in vitro and in vivo stem cell behaviors on PLGA/SL/BMP-2 microspheres are analyzed. Compared with PLGA/BMP-2 microspheres, PLGA/SL/BMP-2 microspheres have significantly higher in vitro and in vivo stem cell attachment, proliferation, differentiation, and matrix mineralization abilities. Therefore, injectable nanoporous PLGA/SL/BMP-2 microspheres can be potentially used as a stem cell platform for bone tissue regeneration. In addition, SL can be potentially used to prepare hydrophilic protein-loaded hydrophobic polymer microspheres with highly entrapped and controlled release of proteins.

1. Introduction

Polymer microsphere-based stem cell delivery systems have been widely designed and studied for stem cell transport to induce neo-tissue regeneration due to their excellent advantages, such as large scale stem cell transport, injectablity, biodegradability, ease of fabrication, drug controlled release capability, and sufficient mechanical properties. Polymers that are used in microsphere-based stem cell delivery systems mainly include poly(lactide-co-glycolide) (PLGA), polylactide, poly(ϵ-caprolactone), polyester, and their mixtures.[1] These polymer microsphere systems have a severe problem that they do not offer a desirable environment for stem cell adhesion and proliferation due to lack of biologically functioncal substances and high hydrophobicity of the microsphere systems. To overcome this problem, biologically functional proteins have been explored to be loaded in the microsphere systems, such as transforming growth

D. Wei, Prof. X. Wang, Prof. J. Zhong
Laboratory of Quality and Safety Risk Assessment for Aquatic Products on Storage and Preservation (Shanghai)
Ministry of Agriculture
Shanghai Engineering Research Center of Aquatic-Product Processing and Preservation
College of Food Science & Technology
Shanghai Ocean University
Shanghai 201306, China
E-mail: jzhong@shou.edu.cn

D. Wei, Prof. J. Zhong
State Key Laboratory of Molecular Engineering of Polymers
Fudan University
Shanghai 200438, China

D. Wei, J. Dao
School of Life Sciences
Tsinghua-Peking Center for Life Sciences
Tsinghua University
Beijing 100084, China

Dr. R. Qiao, Prof. M. Gao, Prof. J. Zhong
CAS Key Laboratory of Colloid, and Interface and Chemical Thermodynamics
Institute of Chemistry
Chinese Academy of Sciences
Beijing 100190, China

Prof. J. Su
School of Pharmacy
Shanghai Jiao Tong University
Shanghai 200438, China

Dr. C. Jiang
Department of Chemistry
Rice University
Houston, TX 77005, USA

The ORCID identification number(s) for the author(s) of this article can be found under https://doi.org/10.1002/smll.201800063.

DOI: 10.1002/smll.201800063

factor,[2] bone morphogenic proteins (BMPs),[3] and lactoferrin.[4] These protein-loaded polymer microsphere systems are not ideal due to the low protein entrapment efficiency.

Generally, ideal biologically functional protein-loaded polymer microsphere system as stem cell platform for cell delivery should possess four pivotal characteristics: (i) high entrapment efficiency of biologically functional proteins in the microspheres; (ii) controlled release of biologically functional proteins from the microspheres; (iii) high stem cell attachment and proliferation abilities due to the controlled release of biologically functional proteins; and (iv) high stem cell differentiation and matrix mineralization abilities due to the controlled release of biologically functional proteins. Because protein molecules are hydrophilic and polymer molecules are hydrophobic, it is difficult to entrap a large number of protein molecules into the core of polymer microspheres, which resulted in low entrapment efficiency of biologically functional proteins in polymer microspheres.[5] Moreover, the release of biologically functional proteins in polymer microspheres showed a high initial protein burst behavior.[6] In addition, acidic groups are present in acidic polymers such as polylactide or in degradation products of many polymers such as PLGA, poly(ϵ-caprolactone), and polyester. These acidic groups will facilitate the denature and decreased bioactivity of protein drugs,[7] which strongly impedes their application in clinics.[8]

Tremendous efforts have been made to prepare ideal biologically functional protein-loaded polymer microsphere system with high entrapment efficiency, controlled release, and high bioactivity of biologically functional proteins. These methods can be classified into four types: (i) Discovery of new polymers and modification of polymers.[2b,9] It is generally time-assuming and not ideal to achieve all the desired properties.[10] In addition, the clinical translation application is also generally time-assuming because these new-developed and modified polymers are needed to be approved by U.S. food and drug administration (FDA) before the clinical translational application compared with other FDA-approved polymers such as PLGA. (ii) Preparation of microporous microsphere system,[3,4,11] which cannot significantly increase entrapment effiency because they only increase surface-to-volume ratio. (iii) Optimization of the preparation parameters,[12] which does not provide significant improvement because they cannot change the physicochemical properties of proteins and polymers. (iv) Use of small molecule charged surfactants such as docusate sodium to form protein/surfactant complexes prior to microsphere emulsion preparation.[5] Though this method provides a controlled release ability of biologically functional proteins from the microspheres, it cannot increase the protein entrapment efficiency of biologically functional proteins in the microsphere. (v) Use of amphiphilic polymers such as poloxamer during microsphere emulsion preparation process, though this method provides a controlled release ability of biologically functional proteins from the microspheres, it reduces the protein encapsulation efficiency.[6] (vi) Use of charge polymer additives such as polyelectrolytes to form protein/polymer complexes prior to microsphere emulsion preparation.[7b,13] Use of polyelectrolytes can provide rather satisfied performance,[7b,13] but introduce potential toxicity.[14] It should be noted that the controlled release behaviors of these developed system were still not ideal because they showed biphasic release behaviors. Therefore, it is necessary to apply better additives to obtain ideal protein-loaded polymer microsphere system.

To explore the possibility of ideal biologically functional protein-loaded polymer microsphere system with high entrapment efficiency, controlled release, and high bioactivity of biologically functional proteins for stem cell delivery, we choose BMP-2 as the typical model biologically functional protein and PLGA as the model polymer for microsphere preparation in this work. BMPs are typical cell growth factors for osteogenic differentiation and can induce the directed differentiation from stem cells to osteoblast cells. It has been widely applied for the clinical application of orthopedics and bone regeneration.[15] PLGA is one of the most applied polymers for preparing microsphere systems in the field of medical applications.[16] Its degradation kinetics can be adjusted by changing monomer sequence and stereochemistry.[17] Phospholipids are small amphipathic molecules and are the main components of cell membranes.[18] In drug delivery field, phospholipids often play a role of intermediary between the water phase and the oil phase (organic phase).[19] Commercial lecithin is a mixture of phospholipids in oil and is generally obtained by water degumming the extracted oil of seeds. It has been widely explored as nutrient for the development of functional foods and applied as emulsifying agent for oil-in-water emulsions.[20] In this work, first soybean lecithin (SL)/BMP-2 complexes were prepared with different weight ratios (4:1, 5:1, and 6:1, named as 4SL/BMP-2, 5SL/BMP-2, and 6SL/BMP-2, respectively), and then they were encapsulated in PLGA-based microspheres using an oil-in-water emulsion-solvent evaporation method. The physicochemical properties, BMP-2 distribution and entrapment, in vitro BMP-2 release, in vitro stem cell attachment and proliferation, in vitro stem cell differentiation, and in vivo stem cell differentiation and matrix mineralization behaviors were further investigated.

2. Results

2.1. Solubility of SL/BMP-2 Complexes

SL/BMP-2 complexes with different weight ratios (4:1, 5:1, and 6:1) were prepared based on a physical blending method. The solubility of SL/BMP-2 complexes and pure BMP-2 in ultrapure water or dichloromethane were measured and shown in **Table 1**. It is obvious that SL/BMP-2 complexes had a much lower solubility in water and a much higher solubility in dichloromethane compared to pure BMP-2. Moreover, with the

Table 1. BMP-2 solubility in SL/BMP-2 complex with different weight ratios (4:1, 5:1, and 6:1) in water and dichloromethane at 25 °C, respectively ($n = 6$).

Samples	Solubility in water [mg mL^{-1}]	Solubility in dichloromethane [mg mL^{-1}]
Pure BMP-2	7.34 ± 0.97	0.02 ± 0.03
4SL/BMP-2	0.28 ± 0.03	2.42 ± 0.31
5SL/BMP-2	0.26 ± 0.02	3.84 ± 0.26
6SL/BMP-2	0.18 ± 0.02	4.10 ± 0.25

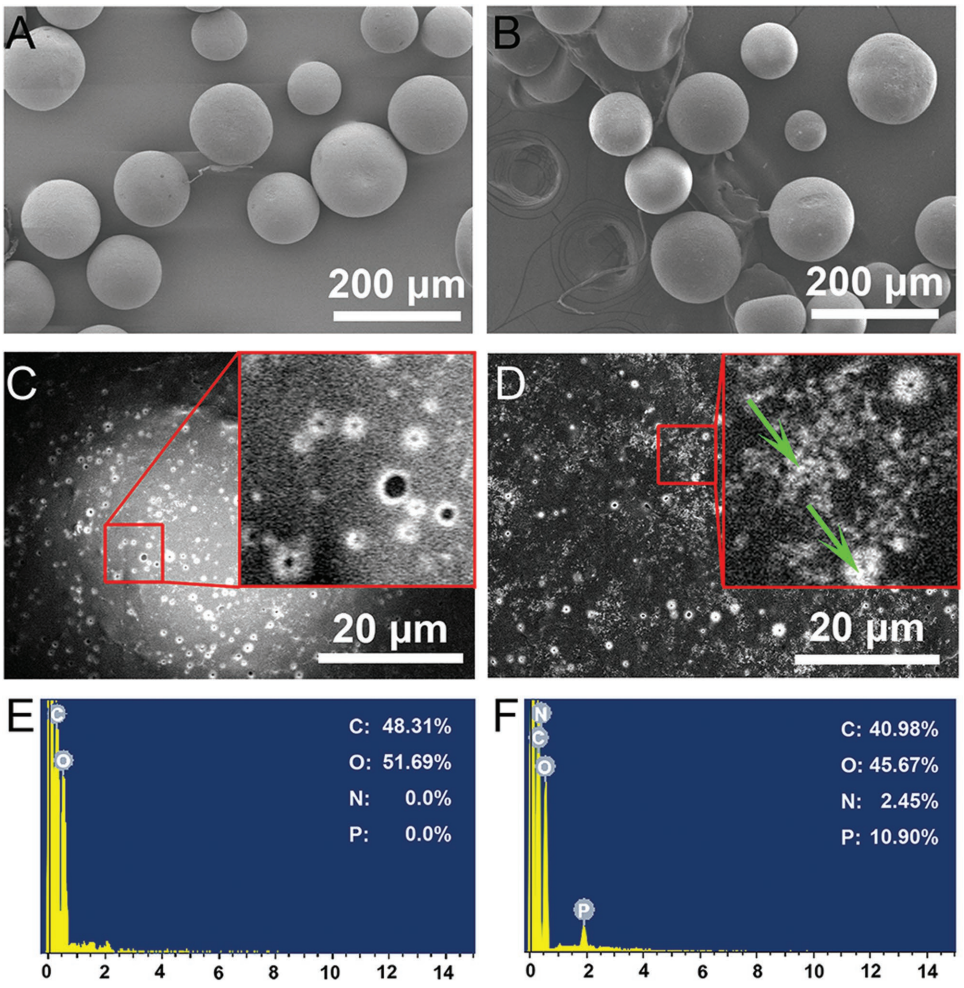

Figure 1. Morphology and element distribution of PLGA-based microspheres. A,C) SEM micrographs of PLGA microsphere. B,D) SEM micrographs of PLGA/6SL/BMP-2 microsphere. E) EDS spectrum of PLGA microsphere. F) EDS spectrum of PLGA/6SL/BMP-2 microsphere.

increase of SL amount, the solubility of SL/BMP-2 complexes in dichloromethane was increased while the solubility in water was decreased.

2.2. Morphology and Confirmation of Nanoporous PLGA-Based Microspheres

PLGA-based microspheres were prepared based on an oil-in-water emulsion-solvent evaporation method. The PLGA-based microspheres were analyzed by scanning electron microscopy (SEM) and energy dispersive spectrometry (EDS), typically as shown in **Figure 1**. The shapes of PLGA-based microspheres were regular and spherical (Figure 1A,B) and the surfaces showed small pores with a diameter of 200–700 nm (Figure 1C,D). The surface of pure PLGA microspheres was smooth (Figure 1C), whereas the surface of PLGA/6SL/BMP-2 microspheres presented a relatively rough surface decorated with SL/BMP-2 complexes (indicated by green arrows in Figure 1D). In addition, less water-filled pores were shown on the surface of PLGA/6SL/BMP-2 microspheres compared with PLGA microspheres. Subsequently, EDS spectra of the PLGA-based microspheres were analyzed. In comparison with the EDS spectrum of PLGA microsphere (Figure 1E), EDS spectrum of PLGA/6SL/BMP-2 microspheres (Figure 1F) showed the presence of P element (10.90%) and N element (2.45%). These results suggest SL/BMP-2 complexes are presented into the water-filled nanopores of PLGA/SL/BMP-2 microspheres.

The average microsphere size and polydispersity index of PLGA-based microspheres were assessed using dynamic light scattering. As shown in **Table 2**, the average sizes of the PLGA-based microspheres were significantly increased after being loaded with SL and SL/BMP-2 complex (from 135.5 μm to 176.6–181.4 μm). Whereas the polydispersity index was in following order: PLGA/SL/BMP-2 (PLGA/4SL/BMP-2, PLGA/5SL/BMP-2, and PLGA/6SL/BMP-2) microspheres > PLGA/BMP-2 microsphere ≈ PLGA/SL microsphere > PLGA microsphere. The increase of the polydispersity index along with the amount of the components in the microsphere system was evident (≈0.1 for single component system, ≈0.12 for two-component systems, and 0.14 for three-component systems), which suggests that the adding of the components can increase the diversity of the microsphere size.

Table 2. Physicochemical properties characterization of PLGA-based microspheres.

PLGA-based microspheres	Average microsphere size [μm]	Polydispersity index	Water uptake [%, $n = 6$]
PLGA microspheres	135.5	0.102	20.0 ± 1.2
PLGA/SL microspheres	177.1	0.117	32.2 ± 9 .1
PLGA/BMP-2 microsphere	171.4	0.123	21.0 ± 1.0
PLGA/4SL/BMP-2 microsphere	176.6	0.142	44.6 ± 6.3
PLGA/5SL/BMP-2 microsphere	178.4	0.141	57.1 ± 11.5
PLGA/6SL/BMP-2 microsphere	181.4	0.146	62.4 ± 9.7

The microspheres can take up water into the nanopores, hence, the hydrophilicity of PLGA-based microspheres can be evaluated or reflected by water uptake rate measurements. The more water uptake, the more hydrophilic the microsphere is. As shown in Table 2, the order of water uptake rates was as follows: PLGA/6SL/BMP-2 microsphere > PLGA/5SL/BMP-2 microsphere > PLGA/4SL/BMP-2 microsphere > PLGA/SL microsphere > PLGA/BMP-2 microsphere ≈ pure PLGA microsphere, which revealed that the SL plays an important role in increasing the hydrophilicity of PLGA-based microspheres. The water uptake changes are resulted from the presence of SL or SL/BMP-2 complex into the nanopores of PLGA-based microspheres.

2.3. Distribution and Entrapment Efficiencies of BMP-2 and SL in Nanoporous PLGA-Based Microspheres

BMP-2 in nanoporous PLGA-based microspheres were immunohistochemically stained using an antibody against BMP-2, as described in previous work.[21] Then, the microspheres were observed by confocal laser scanning microscopy (CLSM), as shown in **Figure 2**A. The fluorescence intensities were quantitatively summarized and compared as shown in Figure 2B,C. The BMP-2 amounts in the section images were more than those in the surface images, which demonstrate that SL/BMP-2 complexes were mainly distributed into the nanocores of PLGA-based microspheres. Further, the BMP-2 entrapment efficiencies of PLGA-based microspheres were evaluated by a modified centrifugation method,[22] as shown in Figure 2D. Both BMP-2 distribution studies and entrapment efficiency studies demonstrated that SL/BMP-2 complexes significantly increased the BMP-2 entrapment amount (from 25.1% to 71.8–83.3%) on the surface and in the nanopores of PLGA-based microspheres. The order of BMP-2 entrapment amount was as follows: PLGA/6SL/BMP-2 microsphere > PLGA/5SL/BMP-2 microsphere > PLGA/4SL/BMP-2 microsphere > PLGA/BMP-2 microsphere, which is similar to the order of water uptake rates (Table 2), the order of solubility in dichloromethane (Table 1), and the reverse order of solubility in water (Table 1). There was a significant difference ($p < 0.05$) between PLGA/4SL/BMP-2 to PLGA/5SL/BMP-2 microspheres, which is also similar to the water uptake rates (Table 2). This work shows PLGA-based microspheres by a two-step method: SL/BMP-2 complex preparation and PLGA/SL/BMP-2 microsphere preparation. Therefore, the more is the SL amount/ratio in SL/BMP-2 complexes, the more solubility is in dichloromethane (the less solubility in water) of SL/BMP-2 complexes, the more entrapment efficiency of SL/BMP-2 complexes is in PLGA/SL/BMP-2 complexes, the more entrapment efficiency of BMP-2 is in PLGA/SL/BMP-2 microspheres, the more hydrophilicity of PLGA/SL/BMP-2 microsphere, and therefore, the more water uptake percentage of PLGA/SL/BMP-2 microsphere.

The SL entrapment efficiencies of PLGA-based microspheres were evaluated by a modified centrifugation method,[22] as shown in Figure 2E. The SL entrapment efficiencies of PLGA-based microspheres were nearly 100%, which confirms that SL has excellent miscibility to PLGA. Considering that the BMP-2 entrapment efficiencies of PLGA/SL/BMP-2 microspheres were not nearly 100%, some SL/BMP-2 complexes (16.7–28.2%) were disassembled during the microsphere preparation process.

2.4. In Vitro Release Behaviors of BMP-2 and SL from Nanoporous PLGA-Based Microspheres

The in vitro BMP-2 and SL release behaviors of PLGA-based microspheres were analyzed. Concerning the in vitro BMP-2 release behaviors, as shown in **Figure 3**A, PLGA/BMP-2 microsphere showed a clearly quick burst release in the first two days with 82.8% cumulative release and a very slow release from day 2 to day 30. It is a typical biphasic behavior, which was previously reported for protein release behavior from PLGA-based microspheres.[6] Actually, the biphasic behavior was characterized by an initial protein burst release followed by a relatively constant release. Considering BMP-2 distribution in nanoporous PLGA/BMP-2 microspheres (Figure 2), the initial BMP-2 burst of PLGA/BMP-2 microsphere corresponds to the release of the BMP-2 molecules on the surface of PLGA-based microspheres and the ones in water-filled nanopores of the microspheres. The second phase can be explained by the release of a few BMP-2 molecules that are entrapped in the matrix of PLGA/BMP-2 microsphere during the process of PLGA microsphere degradation. Because the burst release amount of PLGA/BMP-2 microsphere is more than 80%, this type of biphasic release behavior is not preferred for the clinical application. PLGA/SL/BMP-2 (PLGA/4SL/BMP-2, PLGA/5SL/BMP-2, and PLGA/6SL/BMP-2) microspheres showed a controlled triphasic release behavior. They had a much lower initial burst release in the first day at a range of 20.0–28.0% followed with a slow process from day 2 to day 10 and the cumulative release reached 40.6–62.6%. Finally, the total release amount of BMP-2 reached 44.9–75.8% after 30 d monitoring with a much slower release rate from day 11 to day 30. Moreover, the BMP-2 release amount increased with the increase of SL amount in PLGA/SL/BMP-2 microspheres. Considering BMP-2 distribution in nanoporous PLGA/SL/BMP-2 microspheres (Figure 2), the controlled triphasic release behavior can be explained as below (Figure 3C). The first BMP-2 burst phase corresponds to the release of SL/BMP-2 complexes on the surface of PLGA-based microspheres. The second phase can be explained by the release of SL/BMP-2 complexes in the

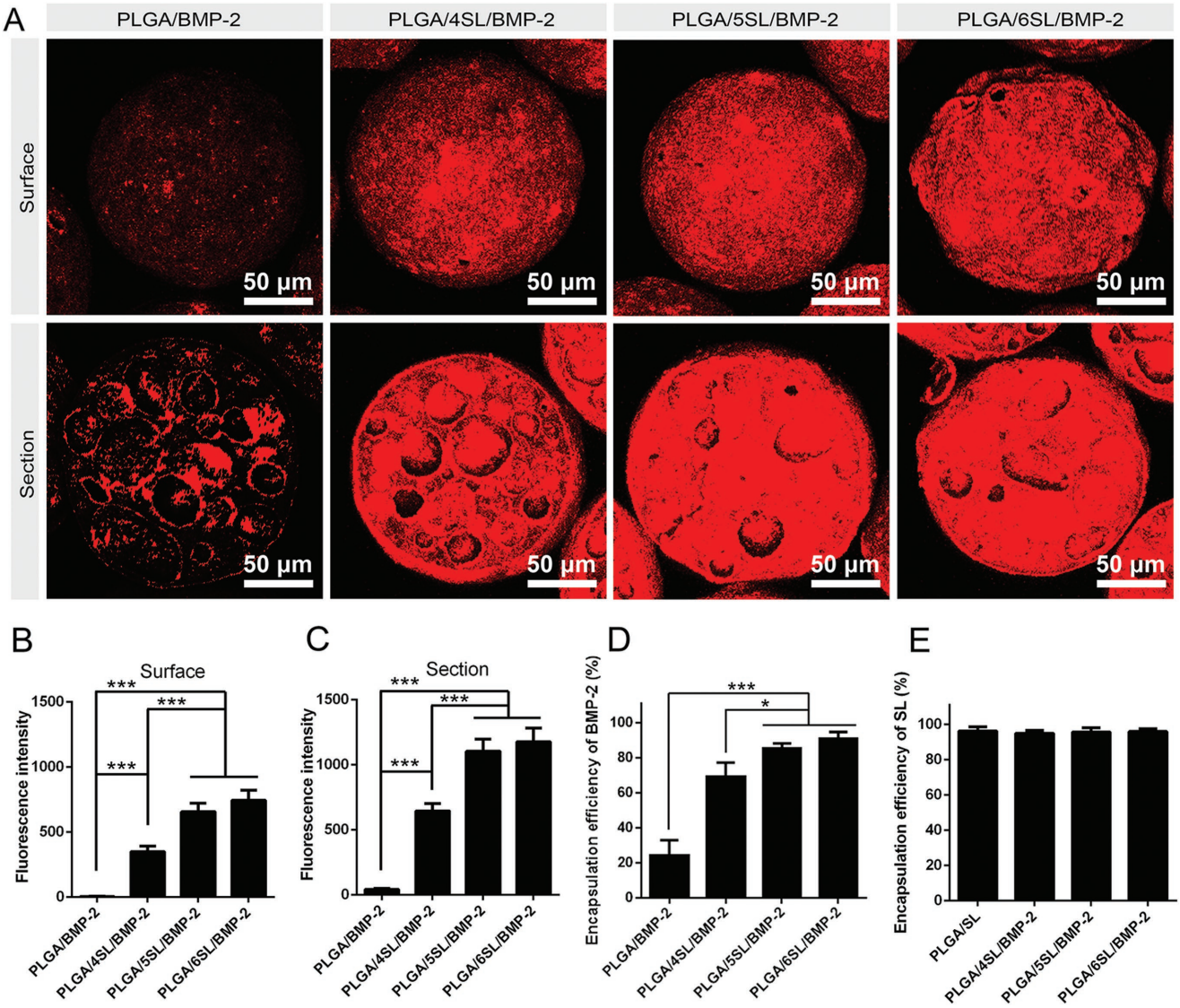

Figure 2. BMP-2 entrapment in PLGA-based microspheres. A) CLSM observation of BMP-2 distribution on the surface (upper row) and section (lower row) of PLGA-based microspheres. B) Fluorescence intensities of BMP-2 distribution on the surface of PLGA-based microspheres. C) Fluorescence intensities of BMP-2 distribution on the section of PLGA-based microspheres. D) Entrapment efficiencies of BMP-2 of PLGA-based microspheres. E) Entrapment efficiencies of SL of PLGA-based microspheres. Statistically significant differences among PLGA-based microspheres: $*p < 0.05$, $**p < 0.01$, $***p < 0.005$, $n = 6$.

water-filled nanopores in the core of PLGA/SL/BMP-2 microspheres. The third phase can be explained by the release of SL/BMP-2 complexes that were entrapped in the matrix of PLGA/SL/BMP-2 microspheres during the microsphere degradation. The controlled triphasic release behaviors is preferred for the clinical application.

The in vitro SL release behaviors showed typical controlled triphasic release behaviors (Figure 3B), which are similar to the in vitro BMP-2 release behaviors from PLGA/SL/BMP-2 microspheres. Moreover, the in vitro SL release percentages of PLGA/SL/BMP-2 microspheres with time were similar and were lower than BMP-2 release percentrages. It might be resulted from that some of SL molecules may be kept in the microspheres during the SL/BMP-2 complex release process at the microsphere–water interface.

2.5. In Vitro Stem Cell Attachment and Proliferation of Human Bone Mesenchymal Stem Cells On Nanoporous PLGA-Based Microspheres

The in vitro stem cell attachment and proliferation of human bone mesenchymal stem cells (hBMSCs) on PLGA-based microspheres were investigated to evaluate the in vitro biological effect of BMP-2 releasing from the current microsphere systems. In general, the hBMSCs were culturing in the solutions of different PLGA-based microspheres and attachment efficiencies were calculated by dividing the number of attached cells on microspheres by the seeding cells after 6 h culturing. As shown in **Figure 4**A, all PLGA-based microspheres allowed hBMSCs adhesion in 6 h. Compared with PLGA and PLGA/SL microspheres, PLGA/BMP-2 microphere slightly increased the

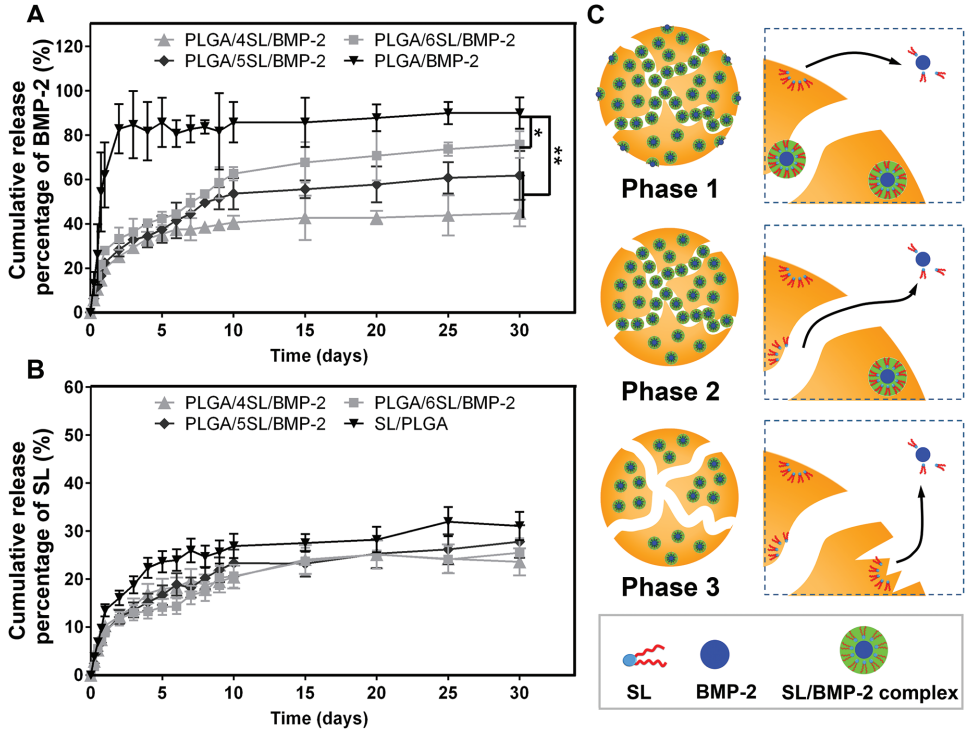

Figure 3. In vitro release behaviors of BMP-2 and SL from PLGA-based microspheres in PBS (pH 7.4) supplemented with 0.1% BSA at 37 °C for 30 d. A) In vitro release behavior of BMP-2. Statistically significant differences among PLGA-based microspheres: $*p < 0.05$, $**p < 0.01$, $n = 3$. B) In vitro release behavior of SL. C) Schematic of in vitro triphasic release behaviors of BMP-2 and SL from PLGA/SL/BMP-2 microspheres. The right images are magnified images from the left images. Some of SL molecules may be kept in the microspheres during the SL/BMP-2 complex release process at the microsphere–water interface.

attachment efficiency and PLGA/SL/BMP-2 microspheres significantly increased the attachment efficiencies. BMP-2 entrapment efficiencies of PLGA/BMP-2, PLGA/4SL/BMP-2, PLGA/5SL/BMP-2, and PLGA/6SL/BMP-2 microspheres were 24.59 ± 8.60%, 69.44 ± 8.01%, 85.66 ± 2.74%, and 90.96 ± 3.96%, respectively (Figure 2D). At the time point of 6 h, the BMP-2 cumulative release percentages of PLGA/BMP-2, PLGA/4SL/BMP-2, PLGA/5SL/BMP-2, and PLGA/6SL/BMP-2 microspheres were 13.07 ± 1.25%, 7.43 ± 2.36%, 6.30 ± 0.99%, and 5.76 ± 0.90%, respectively (Figure 3A). Therefore, the BMP-2 release amounts of PLGA-based microspheres at the time point of 6 h were in following order: PLGA/6SL/BMP-2 microsphere > PLGA/5SL/BMP-2 microsphere > PLGA/4SL/BMP-2 microsphere > PLGA/BMP-2 microsphere. So, more loading and release of BMP-2 can promote the cell attachment of hBMSCs, similarly to previous reports[23] Moreover, with the increase of BMP-2 release amounts, the attachment efficiencies of hBMSCs increased in PLGA-based microspheres, which suggest the released BMP-2 molecules have good bioactivity to assist microspheres to have good cell attachment abilities.

The overall in vitro hBMSCs proliferation was characterized by the CCK-8 assay after 1, 7, and 15 d of culturing in different PLGA-based microspheres medium solutions (Figure 4B). In our experiments, the cell culture medium was replaced with new medium every day. Therefore, the cell proliferation ability of PLGA-based microspheres was dependent on the BMP-2 release amounts and bioactivity every day. As shown in Figure 4B, the cell proliferation abilities on PLGA/SL/BMP-2 microspheres were significantly higher than those on other three types of PLGA-based microsphere at days 1, 7, and 15, which suggests the released BMP-2 molecules have good bioactivity to assist microspheres to have good cell proliferation abilities. It should be noted that PLGA/5SL/BMP-2 microsphere had the best cell proliferation ability among all the PLGA-based microspheres.

Furthermore, the cell proliferation on the surface of the PLGA-based microspheres was investigated by using CLSM. As displayed in Figure 4C, the amounts of hBMSCs stained by green fluorescence on the surface of PLGA/5SL/BMP-2 microsphere were much more than the cells growing on the surface of the PLGA/BMP-2 microsphere, which is consistent with the CCK-8 assay (Figure 4B).

The morphologies of hBMSCs on PLGA/5SL/BMP-2 microspheres were observed after 1, 7, and 15 d of incubation by using SEM (Figure 4D). The attached cells showed spindle or multilateral shapes after 1 and 7 d of incubation. After 15 d of incubation, the micrographs show that hBMSCs on PLGA/5SL/BMP-2 microsphere formed cell populations with high densities, which is similar to the observations from the CLSM results (Figure 4C).

2.6. In Vitro Stem Cell Osteogenic Differentiation Behaviors of hBMSCs on Nanoporous PLGA-Based Microspheres

BMP-2 has been demonstrated to be effective in promoting the osteogenic differentiation. Thus, we further analyzed the

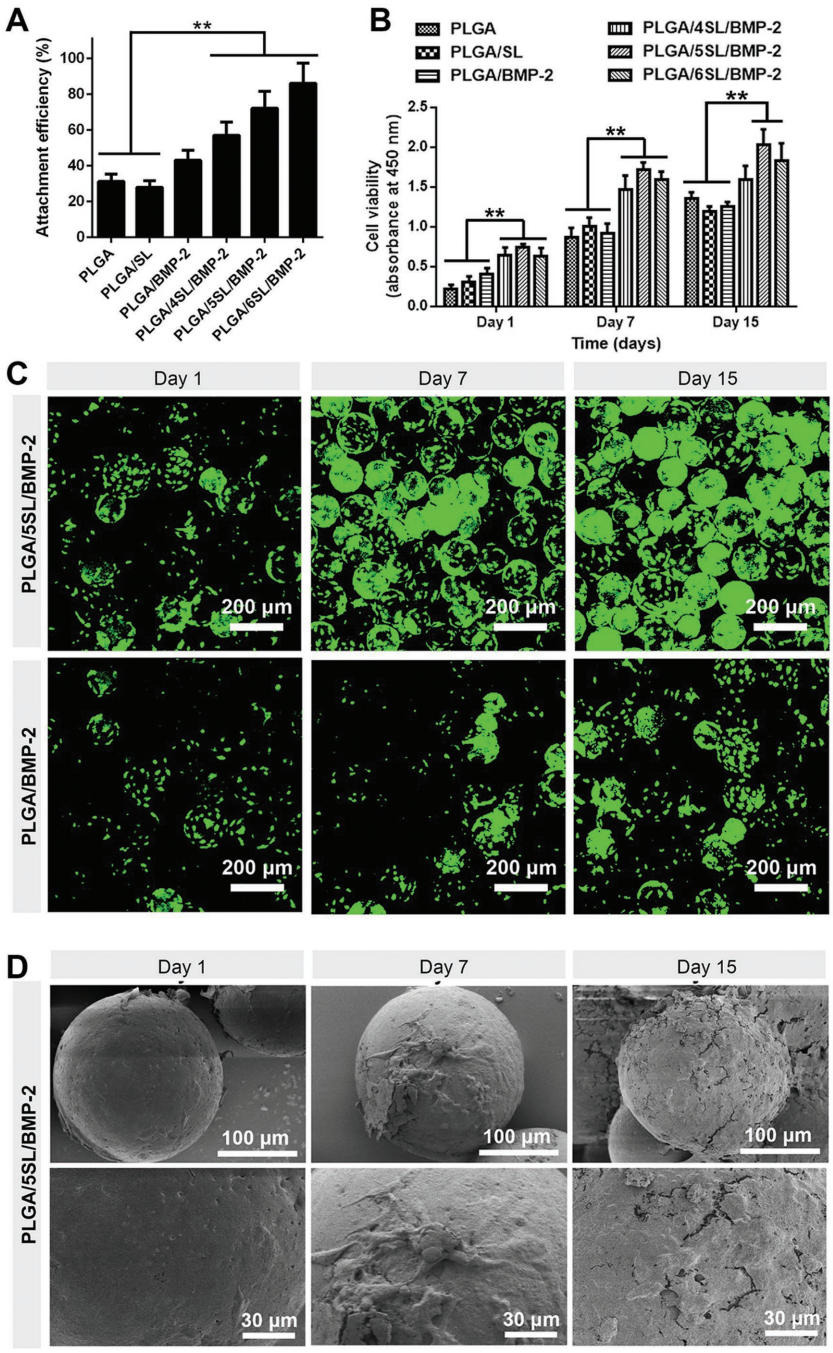

Figure 4. Stem cell attachment and proliferation assays of hBMSCs on PLGA-based microspheres. A) hBMSCs attachment assay on PLGA-based microspheres. B) CCK-8 assays of hBMSCs proliferation on PLGA-based microspheres. Statistically significant differences among PLGA-based microspheres: $^{**}p < 0.01$, $n = 6$. C) CLSM observation of hBMSCs cultured on PLGA/5SL/BMP-2 and PLGA/BMP-2 microspheres at different incubation days. Green colors indicate hBMSCs. D) SE micrographs of hBMSCs cultured on PLGA/5SL/BMP-2 microsphere at different incubation days. The below row are zoomed in images from the upper row.

hBMSCs differentiation on the current PLGA-based microspheres by measuring the alkaline phosphatase (ALP) activity, type I collagen expression, and gene expression markers of hBMSCs incubated with PLGA-based microspheres. As shown in **Figure 5**A, the ALP activity in the PLGA/SL/BMP-2 microspheres was largely increased after 7 and 15 d incubation and showed significant difference to other three types of PLGA-based microspheres. ALP activity in the PLGA/BMP-2 microsphere was also largely increased compared with PLGA and PLGA/SL microspheres. It should be noted that PLGA/5SL/BMP-2 microsphere had the best ALP activity among all the PLGA-based microspheres.

Type I collagen expression of hBMSCs on PLGA-based microspheres at day 15 was observed by CLSM, typically as shown in Figure 5B. PLGA/5SL/BMP-2 microsphere had higher collagen expression than PLGA/BMP-2 microsphere, which is consistent with the ALP activity assay.

There are six kinds of gene expression markers of bone tissue formation: collagen type-1 (COL-1), matrix Gla-protein (MGP), Runt-related transcription factor 2 (RUNX2), osteocalcin (OCN), osteopontin (OPN), and osteoprotegerin (OPG). COL-1,[24] RUNX2,[25] OCN,[26] OPN,[27] and OPG[28] are positively related biomarkers of bone tissue formation. MGP is negatively related biomarker of bone tissue formation.[29] Gene expressions of these osteogenic differentiation markers were assessed using real time polymerization chain reaction (PCR) analysis. The primers used in this work were shown in **Table 3**. As shown in Figure 5C, the gene expression levels of the positively related biomarkers were all upregulated in the SL/BMP-2 complex-loaded PLGA-based microspheres. Meanwhile, the negatively related biomarker MGP was down-regulated in those groups.

All the ALP activity, type I collagen expression, and the gene expression analysis confirmed PLGA/SL/BMP-2 microspheres had better in vitro cell differentiation abilities of hBMSCs compared with others. It should be noted that PLGA/5SL/BMP-2 microsphere had the best in vitro stem cell differentiation ability.

2.7. In Vivo Heterotopic Bone Formation Assay of hBMSCs-Loaded PLGA-Based Microspheres

According to above results, though the entrapment efficiency of BMP-2 and the stem cell attachment efficiency increased with the increase of SL amount in PLGA/SL/BMP-2 microspheres, PLGA/5SL/BMP-2 microsphere had the best stem cell proliferation and differentiation abilities. It suggests the presence of excessive SL/BMP-2 complexes could not increase stem cell proliferation and differentiation abilities, and PLGA/5SL/BMP-2

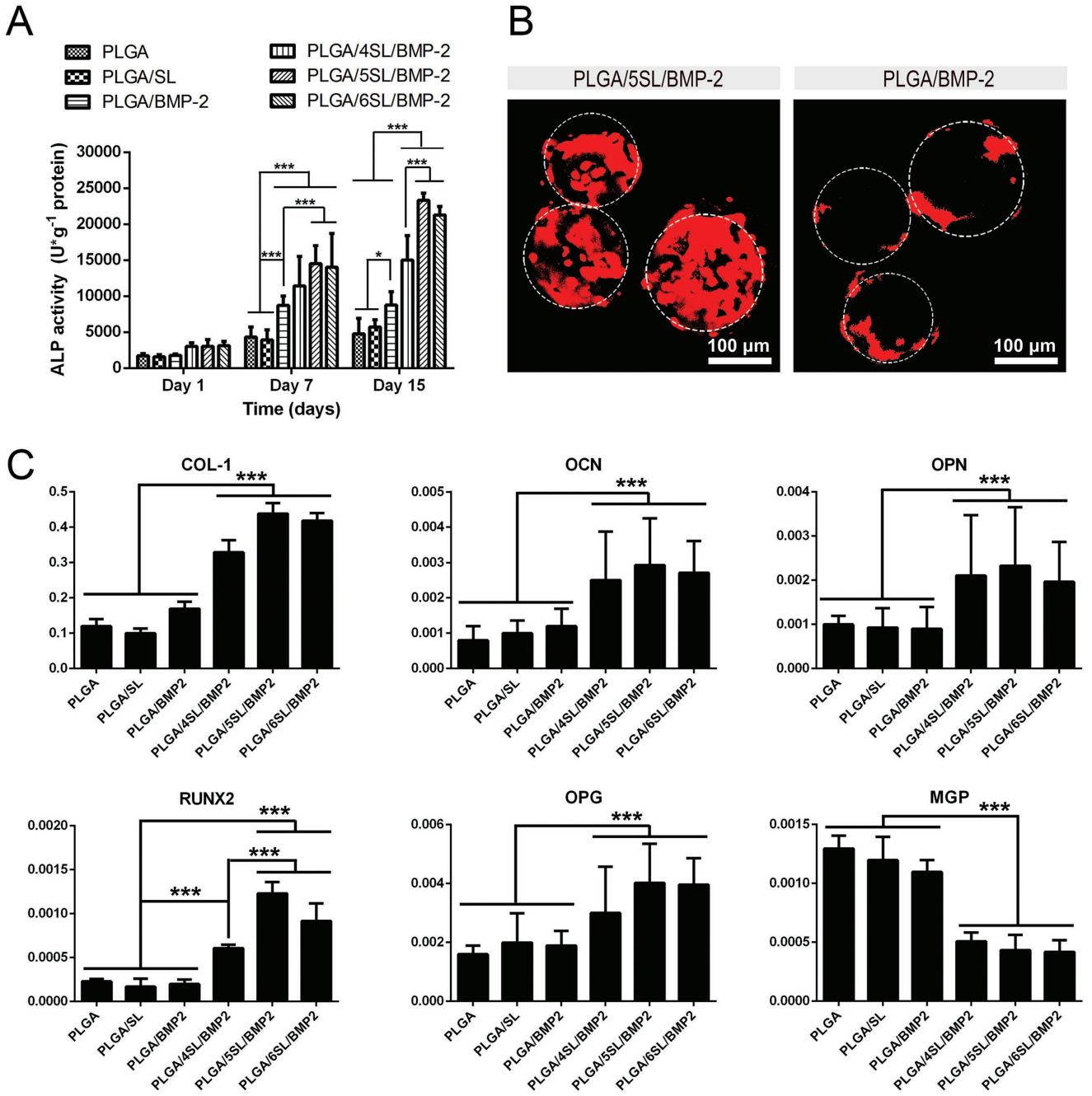

Figure 5. In vitro stem cell differentiation assays of PLGA-based microspheres. A) ALP activity assay of hBMSCs cultured on PLGA-based microspheres at different incubation days. ALP activity was determined as enzyme activity units (U) per gram of protein. Statistically significant difference against the ALP activity of PLGA/BMP-2 microsphere: $*p < 0.05$, $**p < 0.01$, $***p < 0.005$, $n = 6$. B) CLSM observation of Type I collagen distribution on the surface of PLGA/5SL/BMP-2 and PLGA/BMP-2 microspheres at day 15. C) Quantitative PCR analysis of osteogenic gene markers expression in hBMSCs cultured on PLGA-based microspheres at day 15. The *y*-axis represents the relative expression ($2^{-\Delta CT}$) normalized to the expression level of the housekeeping gene *β*-actin. Statistically significant differences among PLGA-based microspheres: $*p < 0.05$, $***p < 0.005$, $n = 3$.

microsphere might be the most suitable system for stem cell proliferation and differentiation. Therefore, we subcutaneously injected hBMSCs-loaded PLGA/5SL/BMP-2 and PLGA/BMP-2 microspheres into the back of nude mice for in vivo heterotopic bone formation assay (**Figure 6**B). Then, hematoxylin and eosin (H&E) staining was applied to analyze cell dist ribution and cell density. H&E staining results showed hBMSCs grew well around both PLGA/5SL/BMP-2 and PLGA/BMP-2 microspheres at weeks 1 and 8 (Figure 6A). Masson's trichrome staining was applied to analyze collagen expression at weeks 1 and 8 (Figure 6A). It showed that more collagen organization (blue color) was present in PLGA/5SL/BMP-2 microsphere in comparison with PLGA/BMP-2 group. OCN staining was applied to analyze stem cell osteogenic differentiation abilities

Table 3. Primer sequences used for RT-PCR analysis in this study.

Genemarkers	Primer sequences	
	Forward	Reverse
Collagen type-1	5′-GACGAAGACATCCCACCAAT-3′	5′-AGATCACGTCATCGCACAAC-3′
Matrix Gla-protein	5′-CAAGAGAGGATCCGAGAACG-3′	5′-CGCTTCCTGAAGTAGCGATT-3′
Runt-related transcription factor 2	5′-CCCAGATCATGTTTGAGACCT-3′	5′-CCTCGTAGATGGGCACAGT-3′
Osteocalcin	5′-GTGCAGCCTTTGTGTCCAA-3′	5′-GCTCACACACCTCCCTCCT-3′
Osteopontin	5′-ACTGATTTTCCCACGGACCT-3′	5′-TCAGGGTACTGGATGTCAGG-3′
Osteoprotegerin	5′-GGGGACCACAATGAACAACT-3′	5′-AGCTGATGAGAGGTTTCTTCG-3′

of PLGA-based microspheres. OCN staining results showed PLGA/5SL/BMP-2 microsphere had significantly better osteogenic differentiation ability than PLGA/BMP-2 microsphere (Figure 6A). According to the results from H&E staining, Masson's trichrome staining, and OCN staining,no obvious morphological changes of the PLGA-based microspheres were observed at week 1. But at week 8, some PLGA-based microspheres were deformed (indicated by asterisk) and some gaps (indicated by arrows) were present in the PLGA-based microspheres. It suggested that the PLGA microspheres slowly degradated in the in vivo heterotopic bone formation process. It is also consistent with our in vitro degradation results of PLGA-based microspheres (data not shown) and other group's results.[30] Micro-CT was applied to analyze matrix mineralization abilities of PLGA-based microspheres. Micro-CT results showed PLGA/5SL/BMP-2 microsphere had significantly higher ratio of new bone volume to existing tissue volume (BV/TV) and bone mineral density (BMD) values than PLGA/BMP-2 microsphere (Figure 6C,D). Moreover, reconstructed 3D micro-CT images (Figure 6E) also confirmed this point.

To further determine the ossify ability during in vivo heterotopic bone formation process, total RNA in the newly formed tissues with implanted microspheres at week 8 was isolated and was examined by quantitative real-time polymerization chain reaction (qRT-PCR). Similarly to qRT-PCR results of in vitro stem cell differentiation assays (Figure 5C), qRT-PCR results of in vivo heterotopic bone formation experiments (**Figure 7**) showed that the gene expression levels of the positively related biomarkers (COL-1, OCN, OPN, RUNX2, and OPG) were all upregulated and the gene expression level of the negatively related biomarker (MGP) was downregulated in the PLGA/5SL/BMP-2 group in comparison with the PLGA/BMP-2 group.

All the in vivo heterotopic bone formation results demonstrate PLGA/5SL/BMP-2 microsphere had significantly better in vivo stem cell osteogenic differentiation and matrix mineralization abilities than PLGA/BMP-2 microsphere. The high bioactivity of controlled released BMP-2 from PLGA-based

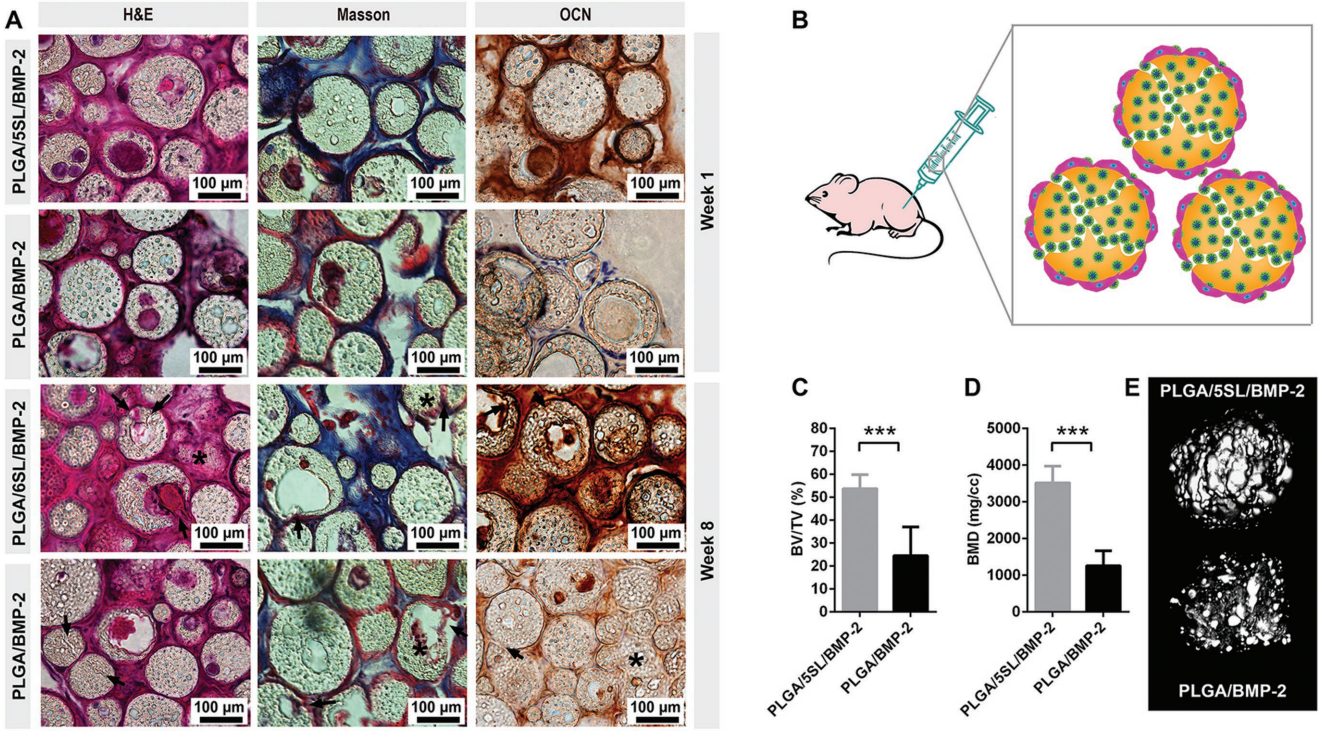

Figure 6. In vivo heterotopic bone formation assay. A) H&E staining, Masson's trichrome staining, and OCN staining of hBMSCs on PLGA-based microspheres. Asterisks indicate deformed microspheres and arrows indicate gaps in the microspheres. B) Schematics of the in vivo hBMSCs-loaded PLGA-based microspheres implantation. After hBMSCs seeding on PLGA-based microspheres for 7 d, the microspheres were implanted subcutaneously on the back of of 5-week-old BALB/c homozygous nude (nu/nu) mice. C) Percentages of new BV/TV of implanted microspheres. D) BMD of implanted microspheres. E) Reconstructed 3D micro-CT images of implanted microspheres. Statistically significant differences among PLGA-based microspheres: ***$p < 0.005$, $n = 3$.

microspheres for stem cell attachment, proliferation, osteogenic differentiation, and matrix mineralization can be proposed as showed in **Figure 8**. Compared with PLGA/BMP-2 microsphere, PLGA/SL/BMP-2 microspheres had significantly higher stem cell attachment ability, higher stem cell proliferation ability, higher stem cell differentiation, and matrix mineralization abilities due to triphasic controlled released BMP-2 from microspheres with highly entrapped BMP-2.

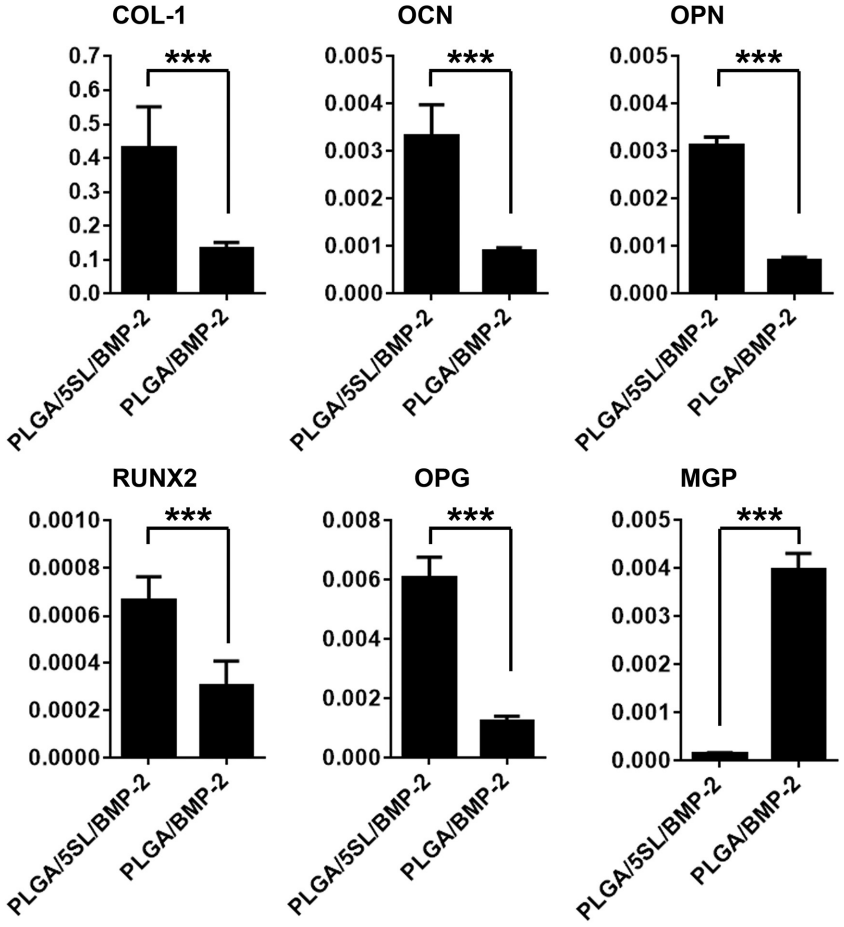

Figure 7. Quantitative PCR analysis of osteogenic gene markers expression of newly formed tissue in mice on week 8. The *y*-axis represents the relative expression ($2^{-\Delta CT}$) normalized to the expression level of the housekeeping gene β-actin. Statistically significant differences among PLGA-based microspheres: ***$p < 0.005$, $n = 3$.

3. Conclusion

Injectable scaffolds such as PLGA microspheres have obtained much attention for bone regeneration due to their wide application potential such as easy filling of scaffolds with osteogenic cells for irregularly shaped bone defects through minimally invasive surgery,[31] and easy implantation of scaffolds with osteogenic cells for large bone defect regeneration through traditional surgical treatment.[32] Theoretially, for large bone defect regeneration, in this work, injectable nanoporous PLGA/SL/BMP-2 microspheres were prepared by a two-step method: SL/BMP-2 complexes preparation and PLGA/SL/BMP-2 microspheres preparation. According to above results, compared with PLGA/BMP-2 microsphere, PLGA/SL/BMP-2 microspheres had significantly higher BMP-2 entrapment efficiency (Figure 2), significantly more controlled BMP-2 release ability (Figure 3), significantly higher stem cell attachment and proliferation abilities (Figure 4), significantly higher in vitro and in vivo stem cell differentiation, and matrix mineralization abilities (Figures 5 and 6). The excellent stem cell attachment, proliferation, differentiation, and matrix mineralization abilities of PLGA/SL/BMP-2 microspheres resulted high BMP-2 entrapment efficiency, controlled BMP-2 release, and high bioactivity of released BMP-2. These excellent behaviors were attributed to the application of SL to form stable SL/BMP-2 complex for the preparation of PLGA/SL/BMP-2 microspheres. This work suggests that injectable nanoporous PLGA/SL/BMP-2 microspheres can be potentially used as stem cell platform for bone tissue regeneration. Moreover, SL can be potentially used to prepare hydrophilic protein-loaded hydrophobic polymer microspheres with highly entrapped and controlled released proteins.

4. Experimental Section

Materials: PLGA (50:50) with an inherent viscosity of 0.18–0.25 dL g^{-1} was bought from Jinan Daigang Biomaterial Co., Ltd. (Shandong, China). Recombinant human BMP-2 was purchased from R&D Systems (Minneapolis, MN, USA). SL containing 70–97% phosphatidylcholine was bought from Shanghai Tai-wei Pharmaceutical Co. Ltd. (Shanghai, China). Poly(vinyl alcohol) (PVA, 87–89% hydrolyzed with an average M_w of 13 000–23 000) was purchased from Sigma-Aldrich, USA. All of the general chemicals were of analytical grade and were bought from Sinopharm Chemical Reagent Co., Ltd. (Shanghai, China).

Preparation of SL/BMP-2 Complexes: SL/BMP-2 complexes were prepared based on a physical blending method. Briefly, SL and BMP-2 with different weight ratios (4:1, 5:1, and 6:1) were dissolved in dimethyl sulfoxide containing 5% (v/v) acetic acid by slow magnetic stirring at 30 °C for 24 h. Then, the mixture was lyophilized for 12 h to remove the solvent. The lyophilized SL/BMP-2 complexes were hermetically-sealed and stored at 4 °C for further use.

Solubility Studies of SL/BMP-2 Complexes: Solubility studies of SL/BMP-2 complexes were performed in ultrapure water or dichloromethane. Briefly, excess SL/BMP-2 complexes were added in ultrapure water or dichloromethane in sealed glass containers. Then, the containers were gently shaken on an orbital shaker at 25 °C for 24 h. Subsequently, the samples were centrifuged at 6000 rpm for 10 min. The resultant supernatant was taken out for further analysis. For the solubility measurement of SL/BMP-2 complexes in ultrapure water, BMP-2 was determined by a human BMP-2 Quantikine ELISA kit (Shanghai Kejian biotechnology Co., Ltd, China). For the solubility measurement of SL/BMP-2 complexes in dichloromethane, the dichloromethane in the collected supernatant was evaporated to obtain dry SL/BMP-2 complexes. Subsequently, dry SL/BMP-2 complex powder was dissolved

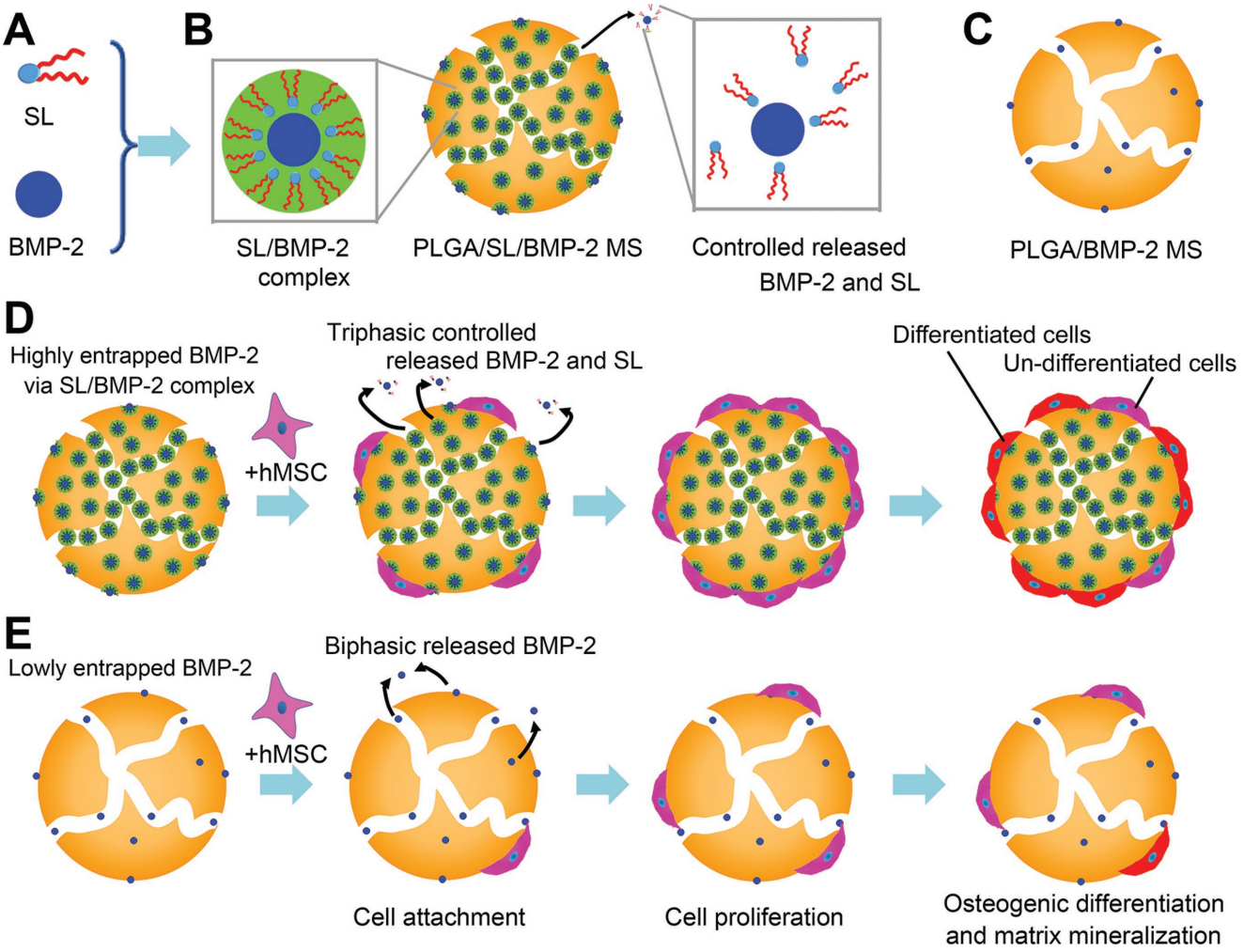

Figure 8. Proposed mechanism of stem cell attachment, proliferation, osteogenic differentiation, and matrix mineralization on PLGA-based microspheres. A) Cross-section schematic of SL and BMP-2. B) Cross-section schematic of SL/BMP-2 complex, PLGA/SL/BMP-2 microspheres, and controlled released BMP-2 and SL from PLGA/SL/BMP-2 microspheres. C) Cross-section schematic of PLGA/BMP-2 microsphere. D) Cross-section schematic of hBMSCs cultured on PLGA/SL/BMP-2 microspheres with a triphasic release behavior of BMP-2 and SL. BMP-2 is highly loaded in PLGA/SL/BMP-2 microspheres. E) Cross-section schematic of hBMSCs cultured on PLGA/BMP-2 microspheres with a biphasic release behavior of BMP-2. BMP-2 is lowly loaded in PLGA/BMP-2 microspheres. Compared with PLGA/BMP-2 microspheres, PLGA/SL/BMP-2 microspheres significantly increase hBMSCs attachment, proliferation, osteogenic differentiation, and matrix mineralization.

in ultrapure water. Finally, BMP-2 was determined by the ELISA Kit. Six parallel experiments were performed for each sample.

Preparation of PLGA-Based Microspheres: PLGA/SL/BMP-2 microspheres were prepared based on an oil-in-water emulsion-solvent evaporation method. SL/BMP-2 complexes (0.01 g BMP-2) and 0.25 g PLGA were dissolved in 5 mL dichloromethane. 0.1 g PVA was dissolved into 100 mL ultrapure water (0.1%, w/v) by slow magnetic stirring at 80 °C for 2 h. At room temperature, the 5 mL dichloromethane solution (SL/BMP-2 complexes and PLGA) was emulsified in 100 mL PVA aqueous solution by magnetic stirring at 150 rpm. Subsequently, the resultant microemulsion was stirred for 12 h at room temperature to evaporate dichloromethane. After that, the resultant PLGA/SL/BMP-2 microspheres were centrifuged at 800 rpm for 5 min and the supernatant was removed. The precipitation was washed three times with ultrapure water by centrifugation to remove residual PVA and stored at 4 °C for further use. PLGA/BMP-2 microsphere, PLGA/SL microsphere, and pure PLGA microsphere were prepared according to the same procedure without the use of SL, BMP-2, and SL/BMP-2 complex, respectively.

Morphology and Size Measurements of PLGA-Based Microspheres: The morphology of PLGA-based microspheres was observed by a SEM (Hitachi, S-4800, Japan) at an accelerated voltage of 5 kV. Element (C, N, O, and P) distribution was examined using an EDS (Oxford Instruments, IE250X-Max50, UK).[16] Mastersizer 2000 (Malvern, UK) was employed to analyze the mean microsphere size and distribution of the PLGA-based microspheres at room temperature. The mean particle size was displayed by intensity distribution and was evaluated by polydispersity index.

Water Uptake Rate Measurements of PLGA-Based Microspheres: Hydrophilicity of PLGA-based microspheres was analyzed by measuring the water uptake rate.[16] The PLGA-based microspheres were lyophilized for 12 h. The dried PLGA-based microspheres were immersed in ultrapure water at room temperature for 72 h. After that, the excess water was removed by filter paper. The water uptake rate of the PLGA-based microspheres was calculated according to the following Equation (1)

$$\text{Water uptake rate}(\%) = (W_{\text{after}} - W_{\text{before}})/W_{\text{before}} \times 100\% \quad (1)$$

where W_{before} and W_{after} are the masses of the microspheres before and after the immersion in water, respectively. Six parallel experiments were performed for each sample.

Distribution of BMP-2 in PLGA-Based Microspheres: Microsphere samples were fixed with 4% paraformaldehyde for 30 min, permeabilized with 0.1% Triton X-100 for 15 min, and then blocked with 3% bovine serum albumin (BSA; Sigma-Aldrich) for 30 min. Then, microsphere samples were incubated with primary antibody (rabbit anti-human BMP-2, Invitrogen, USA) at 4 °C overnight and incubated in the specified secondary antibodies (Alex555-conjugated rat anti-rabbit, Invitrogen, USA) for 1 h. Images were captured and analyzed with a CLSM (Nikon, Japan). The distribution of BMP-2 on microspheres surfaces was showed by a 3D reconstruction image from serial sections at the interval of 5 μm. In order to analyze BMP-2 distribution on the section of microspheres, the section of microspheres was prepared by scalpel prior to the immunohistochemical staining process of BMP-2. After staining, the section of microspheres was imaged by CLSM.

Entrapment Efficiency Measurements of PLGA-Based Microspheres: The BMP-2 and SL entrapment efficiencies of PLGA-based microspheres were evaluated by a modified centrifugation method.[22] Briefly, during the preparation process of PLGA-based microsphere, the supernatant after centrifugation was collected for free BMP-2 and SL measurement (W_{free}). The free BMP-2 and SL amounts in the supernatant, which were not packaged into microspheres, were analyzed by the human BMP-2 Quantikine ELISA kit and a phospholipid assay kit (MERCK, Germany), respectively. Equal SL/BMP-2 complex was dissolved in 100 mL 0.1% PVA solution, and then was subjected to the same procedure. After that, the active BMP-2 and SL contents were measured by the human BMP-2 Quantikine ELISA kit and the phospholipid assay kit, respectively. The obtained results were defined as total amount of BMP-2 or SL (W_{total}). Therefore, the entrapment efficiency could be calculated through the following Equation (2)

$$\text{Entrapment efficiency}(\%) = (W_{total} - W_{free})/W_{total} \times 100\% \quad (2)$$

Six parallel experiments were performed for each sample.

In Vitro BMP-2 and SL Release Studies of PLGA-Based Microspheres: To perform the BMP-2 and SL release studies,[16] 10 mg PLGA/SL/BMP-2 microspheres were immersed in 300 μL release medium, which was phosphate buffer solution (PBS) (pH 7.4) supplemented with 0.1% BSA (MERCK, Germany). The solutions were incubated on a shaker at 50 rpm at 37 °C for 30 d. The incubation solution was collected and replaced with 300 μL fresh release medium at designateds time points. The amount of released BMP-2 in the collected release medium was determined by the human BMP-2 Quantikine ELISA kit. PLGA/BMP-2 microsphere was applied as the control. Similarly to BMP-2, the released SL was detected by a phospholipid assay kit (MERCK, Germany) and PLGA/SL microsphere was used as the control. Six parallel experiments were performed for each sample.

Cell Culture on PLGA-Based Microspheres: hBMSCs were applied to study the cell attachment, proliferation, and differentiation abilities of PLGA-based microspheres. The hBMSCs are derived from osteocalcin promoter-driven SV-40 T-antigen transgenic mouse calvarias and supplied by the Institute of Biochemistry and Cell Biology, Chinese Academy of Sciences (Shanghai, China). hBMSCs were incubated at 37 °C in in a 5.0% carbon dioxide incubator. 10 mg PLGA-based microspheres were sterilized by 75% ethanol for 1 h. Then they were washed with PBS (pH 7.4) three times by centrifugation. The hBMSCs suspension, containing 1×10^5 cells, was incubated with the PLGA-based microspheres, and then was cultured in a 5% CO_2 incubator at 37 °C. The cell culture media were replaced with new media every day.

Cell Attachment Efficiency Measurement of PLGA-Based Microspheres: Cell attachment efficiencies were assessed according to a previous study.[16] Briefly, at 6 h after the hBMSCs culture with PLGA-based microspheres, the microspheres with attached hBMSCs were collected by a 40 μm sterile cell strainer (Biologix Group Ltd., China) and washed with PBS three times to remove unattached cells. The cells attached on the microspheres were digested by trypsin/ethylene diamine tetraacetic acid, and counted by hemocytometer. Finally, the cell attachment efficiency was calculated according to the following equation

$$\text{Cell attachment efficiency}(\%) = (N_{attached}/N_{total}) \times 100\% \quad (3)$$

where $N_{attached}$ and N_{total} are the numbers of cells attached on microspheres and of seeded cells, respectively. Six parallel experiments were performed for each sample.

Cell Proliferation on PLGA-Based Microspheres: The hBMSCs viability on PLGA-based microspheres was assessed using a CCK-8 assay.[33] Briefly, at the designated time points (1, 7, and 15 d), the culture medium was removed and 2 mL fresh Dulbecco's modified Eagle medium (DMEM) containing 0.2 mL CCK-8 solution was added to each sample. The samples were then incubated at 37 °C for 2 h. All microspheres must be immersed in DMEM medium. 100 μL aliquots of supernatant were transferred into a 96-well plate. The absorbance was measured at 450 nm by a microplate reader (Multiskan MK3, Thermo Labsystems, Finland). Six parallel experiments were performed for each sample.

The distribution patterns of the hBMSCs on PLGA-based microspheres were observed by CLSM.[34] Briefly, at the designated time points (1, 7, and 15 d), the culture medium was removed and 2 mL fresh medium containing 50 ng mL^{-1} fluorescein diacetate (Sigma-Aldrich, USA). The samples were incubated at 37 °C for 10 min. The microspheres were then washed with PBS three times by centrifugation and observed under a confocal laser scanning microscope (Leica, TCS SP5, Germany). The living cells were labeled by fluorescein diacetate. Fluorescein diacetate can penetrate through the living cell membrane and can be hydrolyzed to produce green fluorescein. The distribution of hBMSCs on microspheres surfaces was showed by a 3D reconstruction image from serial sections at the interval of 5 μm. Six parallel experiments were performed for each sample.

Cell morphologies were observed by SEM according to our previous study.[33] Briefly, at the designated time points (1, 7, and 15 d), the microspheres with cells were collected by centrifugation (800 rpm, 5 min). Then they were washed with PBS by centrifugation three times. After that, they were fixed with 2.5% glutaraldehyde for 24 h at 4 °C. Subsequently, the fixed cells were dehydrated through a series of graded alcohols. Finally, the cells were dried for 12 h and observed with a scanning electron microscope (Hitachi S-4800, Tokyo, Japan). Three parallel experiments were performed for each sample.

In Vitro Stem Cell Differentiation Ability Assay: ALP expression in hBMSCs cultured on PLGA-based microspheres was quantitatively analyzed.[35] Briefly, at the designated time points (1, 7, and 15 d), the microspheres with cells were collected by centrifugation (800 rpm, 5 min). Then they were washed three times with PBS by centrifugation. After that, they were suspended in 0.1% Triton X-100 for 10 min. Subsequently, they were centrifuged and the supernatants were collected. According to the protocols of the manufacturers, the ALP activity and the total protein content in the supernatants were measured by an ALP activity kit (Shanghai Fusheng Biotechnology Development Co., Ltd, Shanghai, China) and a protein assay kit (Tiangen, Beijing, China), respectively. Six parallel experiments were performed for each sample.

Expressed COL-1 in hBMSCs on microspheres were evaluated by immunohistochemical analysis. Microspheres samples at 15 d were fixed with 4% paraformaldehyde for 30 min, permeabilized with 0.1% Triton X-100 for 15 min, and then blocked with 3% BSA for 30 min. After that, microspheres samples were incubated with primary antibody (rabbit anti-human COL-1, Invitrogen, USA) at 4 °C overnight and incubated in the specified secondary antibodies (Alex555-conjugated rat anti-rabbit, Invitrogen, USA) for 1 h. The distribution of type I collagen on microspheres surfaces was observed by CLSM (Nikon, Japan) and was showed by a 3D reconstruction image from serial sections at the interval of 5 μm.

To investigate differentiation and matrix mineralization of hBMSCs on PLGA-based microspheres, the expression levels of osteogenic genes at 15 d after cell seeding were estimated by qRT-PCR analysis.[36] Using the QuantiTect SYBR Green PCR kit (Qiagen, Hilden, Germany), we analyzed six kinds of gene markers: COL-1, MGP, RUNX2, OCN, OPN, and OPG. β-actin was applied as housekeeping gene. The sequences of the primers were shown in Table 3. According to the instruction of the PCR Kit, 1 mg of the total RNA of cells for each PLGA-based microspheres was purified

to synthesize the complementary DNA (cDNA). Six parallel experiments were performed for each sample.

In Vivo Microsphere Implantation and Animal Cultivation: The hBMSCs were seeded on PLGA-based microspheres and in vitro cultivated for 7 d before the in vivo study. The PLGA-based microspheres with hBMSCs were implanted subcutaneously on the back of 5-week-old BALB/c homozygous nude (nu/nu) mice (five mice per group) together, as described previously.[37] Implanted samples were harvested after 2 months and fixed in 4% paraformaldehyde for further study. Mice were bred and maintained in the animal care facility at Center of Biomedical Analysis in Tsinghua University. All animal protocols used in this study were approved by the IACUC (Institutional Animal Care and Use Committee) of Tsinghua University and performed in accordance with guidelines of the IACUC. The laboratory animal facility has been accredited by AAALAC (Association for Assessment and Accreditation of Laboratory Animal Care International).

H&E Staining, Masson's Trichrome Staining, and Immunohistochemical Analysis of OCN: After paraformaldehyde treatment, the implant samples were decalcified in 10% ethylene diaminetetraaceticacid (pH 7.4) for 1 week, followed by dehydrationand embedding in paraffin. Sections were cut for Masson's trichrome staining by Trichrome Stain (Masson) kit (Thermo Fisher Scientific, USA) and H&E staining, as described previously.[37a] Meanwhile, OCN expression of these sections was also evaluated by immunohistochemical analysis, as described previously.[37b] The sections were blocked with 3% BSA for 30 min and then incubated with primary antibody against OCN (Thermo Fisher Scientific, USA) at 4 °C overnight. And then the sections were observed with optical microscope (IX83, Olympus, Japan).

Micro-CT Analysis: Micro-CT analysis of implanted samples was performed using a high-resolution Inveon Micro-CT system (Siemens, Germany).[38] The X-ray source was set at a node current of 500 μA and 80 kV, with an exposure time of 500 ms for each of the 360 rotational steps. Image slices were then reconstructed using micro-CT image analysis software (Inveon Research Workplace). The 3D reconstruction and volume quantification of the implant ectopic bone were performed using standardized thresholds. The region of interest was selected, and the lower and upper threshold values for bone were set. The BMD (mg cc^{-1}) and the ratio of BV/TV were calculated by this software.

qRT-PCR Analysis of Newly Formed Tissues: After 8 weeks postsurgery, the implanted newly formed tissue samples were taken out from mice and were frozen immediately in liquid nitrogen. The samples were kept at −80 °C and then were examined by qRT-PCR, as described previously.[39] The samples were homogenized in TRIzol solution (Invitrogen, USA). Similarly to the in vitro test, six kinds of gene markers (COL-1, OCN, OPN, RUNX2, OPG, and MGP) were analyzed by QuantiTect SYBR Green PCR kit. β-actin was applied as housekeeping gene. The sequences of the primers were shown in Table 3.

Statistical Analysis: All data were expressed as mean value ± standard deviation of the parallel experiments. Statistical comparisons were made using Student's *t*-test. The *p*-value <0.05 was considered to be significant.

Acknowledgements

D.W. and R.Q. contributed equally to this work. This work was supported by research grants from the National Key R&D Program (grant no. 2016YFD0400202-8) and the National High Technology Research and Development Program of China (863 Program 2013AA032203).

Conflict of Interest

The authors declare no conflict of interest.

Keywords

bone regeneration, controlled release, high entrapment, PLGA/soybean lecithin/BMP-2 microspheres, stem cell

Received: January 6, 2018
Revised: March 9, 2018
Published online: April 22, 2018

[1] a) J. W. Kostanski, B. Thanoo, P. P. DeLuca, *Pharm. Dev. Technol.* **2000**, *5*, 585; b) T. Takei, M. Yoshida, Y. Hatate, K. Shiomori, S. Kiyoyama, *Polym. Bull.* **2008**, *61*, 391; c) M. J. Alonso, S. Cohen, T. G. Park, R. K. Gupta, G. R. Siber, R. Langer, *Pharm. Res.* **1993**, *10*, 945; d) J. M. Anderson, M. S. Shive, *Adv. Drug Delivery Rev.* **2012**, *64*, 72.

[2] a) L. D. Solorio, A. S. Fu, R. Hernández-Irizarry, E. Alsberg, *J. Biomed. Mater. Res., Part A* **2010**, *92A*, 1139; b) M. Morille, K. Toupet, C. N. Montero-Menei, C. Jorgensen, D. Noël, *Biomaterials* **2016**, *88*, 60.

[3] B. J. Jeon, S. Y. Jeong, A. N. Koo, B.-C. Kim, Y.-S. Hwang, S. C. Lee, *Macromol. Res.* **2012**, *20*, 715.

[4] S. E. Kim, Y.-P. Yun, K.-S. Shim, K. Park, S.-W. Choi, D. H. Suh, *Colloids Surf., B* **2014**, *122*, 457.

[5] K. Fu, R. Harrell, K. Zinski, C. Um, A. Jaklenec, J. Frazier, N. Lotan, P. Burke, A. M. Klibanov, R. Langer, *J. Pharm. Sci.* **2003**, *92*, 1582.

[6] D. Blanco, M. a. J. Alonso, *Eur. J. Pharm. Biopharm.* **1998**, *45*, 285.

[7] a) F. Kang, G. Jiang, A. Hinderliter, P. P. DeLuca, J. Singh, *Pharm. Res.* **2002**, *19*, 629; b) W. Park, D. Kim, H. C. Kang, Y. H. Bae, K. Na, *Biomaterials* **2012**, *33*, 8848.

[8] a) Y. Fu, L. Du, Q. Wang, W. Liao, Y. Jin, A. Dong, C. Chen, Z. Li, *Pharmazie* **2012**, *67*, 299; b) J. W. Lee, K. S. Kang, S. H. Lee, J. Y. Kim, B. K. Lee, D. W. Cho, *Biomaterials* **2011**, *32*, 744.

[9] a) V. Biju, *Chem. Soc. Rev.* **2014**, *43*, 744; b) M. R. Islam, Y. Gao, X. Li, M. J. Serpe, *J. Mater. Chem. B* **2014**, *2*, 2444; c) G. T. Kirby, L. J. White, C. V. Rahman, H. C. Cox, O. Qutachi, F. R. Rose, D. W. Hutmacher, K. M. Shakesheff, M. A. Woodruff, *Polymers* **2011**, *3*, 571.

[10] N. C. Ngwuluka, Y. E. Choonara, P. Kumar, L. C. du Toit, G. Modi, V. Pillay, *AAPS PharmSciTech* **2015**, *16*, 1377.

[11] S. E. Kim, Y.-P. Yun, K.-S. Shim, K. Park, S.-W. Choi, D. H. Shin, D. H. Suh, *Colloids Surf., B* **2015**, *134*, 453.

[12] Y. Yeo, K. Park, *Arch. Pharmacal Res.* **2004**, *27*, 1.

[13] a) W. Park, K. Na, *Colloids Surf., B* **2009**, *72*, 193; b) E. S. Lee, K.-H. Park, D. Kang, I. S. Park, H. Y. Min, D. H. Lee, S. Kim, J. H. Kim, K. Na, *Biomaterials* **2007**, *28*, 2754; c) J.-H. Kim, A. Taluja, K. Knutson, Y. H. Bae, *J. Controlled Release* **2005**, *109*, 86.

[14] C. Brunot, L. Ponsonnet, C. Lagneau, P. Farge, C. Picart, B. Grosgogeat, *Biomaterials* **2007**, *28*, 632.

[15] E. Groeneveld, E. Burger, *Eur. J. Endocrinol.* **2000**, *142*, 9.

[16] H. Shen, X. Hu, F. Yang, J. Bei, S. Wang, *Acta Biomater.* **2010**, *6*, 455.

[17] M. A. Washington, D. J. Swiner, K. R. Bell, M. V. Fedorchak, S. R. Little, T. Y. Meyer, *Biomaterials* **2017**, *117*, 66.

[18] a) J. Zhong, W. Zheng, L. Huang, Y. Hong, L. Wang, Y. Qiu, Y. Sha, *Biochim. Biophys. Acta* **2007**, *1768*, 1420; b) J. Zhong, *Integr. Biol.* **2011**, *3*, 632; c) J. Zhong, D. He, *Chem. - Eur. J.* **2012**, *18*, 4148.

[19] a) G. Hennere, P. Prognon, F. Brion, I. Nicolis, *Chem. Phys. Lipids* **2009**, *157*, 86; b) H. C. Shum, D. Lee, I. Yoon, T. Kodger, D. A. Weitz, *Langmuir* **2008**, *24*, 7651.

[20] a) G. R. List, in *Polar Lipids*, Elsevier, Urbana, IL **2015**, p. 1; b) D. J. McClements, C. E. Gumus, *Adv. Colloid Interface Sci.* **2016**, *234*, 3.

[21] M.-J. Song, J. Amirian, N. T. B. Linh, B.-T. Lee, *J. Appl. Polym. Sci.* **2017**, *134*, 45186.

[22] Q. Peng, Z. R. Zhang, X. Sun, J. Zuo, D. Zhao, T. Gong, *Mol. Pharm.* **2010**, *7*, 565.
[23] a) A. K. Shah, J. Lazatin, R. K. Sinha, T. Lennox, N. J. Hickok, R. S. Tuan, *Biol. Cell* **1999**, *91*, 131; b) W. Zhang, C. Zhu, Y. Wu, D. Ye, S. Wang, D. Zou, X. Zhang, D. L. Kaplan, X. Jiang, *Eur. Cells Mater.* **2014**, *27*, 1.
[24] A. J. Mieszawska, N. Fourligas, I. Georgakoudi, N. M. Ouhib, D. J. Belton, C. C. Perry, D. L. Kaplan, *Biomaterials* **2010**, *31*, 8902.
[25] K.-S. Lee, H.-J. Kim, Q.-L. Li, X.-Z. Chi, C. Ueta, T. Komori, J. M. Wozney, E.-G. Kim, J.-Y. Choi, H.-M. Ryoo, S.-C. Bae, *Mol. Cell. Biol.* **2000**, *20*, 8783.
[26] P. Hauschka, *Pathophysiol. Haemostasis Thromb.* **1986**, *16*, 258.
[27] A. Boskey, M. Maresca, W. Ullrich, S. Doty, W. Butler, C. Prince, *Bone Miner.* **1993**, *22*, 147.
[28] W. Simonet, D. Lacey, C. Dunstan, M. Kelley, M.-S. Chang, R. Lüthy, H. Nguyen, S. Wooden, L. Bennett, T. Boone, *Cell* **1997**, *89*, 309.
[29] A. F. Zebboudj, M. Imura, K. Boström, *J. Biol. Chem.* **2002**, *277*, 4388.
[30] a) J. M. Anderson, M. S. Shive, *Adv. Drug Delivery Rev.* **1997**, *28*, 5; b) K. Fu, D. W. Pack, A. M. Klibanov, R. Langer, *Pharm. Res.* **2000**, *17*, 100.
[31] S.-W. Kang, H. S. Yang, S.-W. Seo, D. K. Han, B.-S. Kim, *J. Biomed. Mater. Res., Part A* **2008**, *85A*, 747.
[32] M. Li, X. Liu, X. Liu, B. Ge, *Clin. Orthop. Relat. Res.* **2010**, *468*, 1978.
[33] N. Xu, X. Ye, D. Wei, J. Zhong, Y. Chen, G. Xu, D. He, *ACS Appl. Mater. Interfaces* **2014**, *6*, 14952.
[34] X. Liu, D. Wei, J. Zhong, M. Ma, J. Zhou, X. Peng, Y. Ye, G. Sun, D. He, *ACS Appl. Mater. Interfaces* **2015**, *7*, 18540.
[35] L. Lin, R. Hao, W. Xiong, J. Zhong, *J. Biosci. Bioeng.* **2015**, *119*, 591.
[36] X. Qu, Y. Cao, C. Chen, X. Die, Q. Kang, *J. Biomed. Mater. Res., Part A* **2015**, *103*, 2786.
[37] a) C. Jin, L. Jia, Y. Huang, Y. Zheng, N. Du, Y. Liu, Y. Zhou, *Stem Cells* **2016**, *34*, 2707; b) J. S. Park, H. N. Yang, S. Y. Jeon, D. G. Woo, K. Na, K.-H. Park, *Biomaterials* **2010**, *31*, 6239.
[38] Y. Huang, Y. Zheng, L. Jia, W. Li, *Stem Cells* **2015**, *33*, 3481.
[39] J. H. Ye, Y. J. Xu, J. Gao, S. G. Yan, J. Zhao, Q. Tu, J. Zhang, X. J. Duan, C. A. Sommer, G. Mostoslavsky, D. L. Kaplan, Y. N. Wu, C. P. Zhang, L. Wang, J. Chen, *Biomaterials* **2011**, *32*, 5065.